PHYSICAL REVIEW E **73**, 051709 (2006)

Universal mean-field phase diagram for biaxial nematics obtained from a minimax principle

Fulvio Bisi and Epifanio G. Virga
Dipartimento di Matematica and CNISM, Università di Pavia, Via Ferrata 1, 27100 Pavia, Italy

Eugene C. Gartland, Jr.
Department of Mathematical Sciences, Kent State University, Kent, Ohio 44242, USA

Giovanni De Matteis and André M. Sonnet
Department of Mathematics, University of Strathclyde, Livingstone Tower, 26 Richmond Street, Glasgow G1 1XH, Scotland

Georges E. Durand
Laboratoire de Physique des Solides Associé au CNRS (LA2), Université Paris Sud, F-91405 Orsay Cedex, France
(Received 16 November 2005; revised manuscript received 13 January 2006; published 19 May 2006)

We study a class of quadratic Hamiltonians which describe both fully attractive and partly repulsive molecular interactions, characteristic of biaxial liquid crystal molecules. To treat the partly repulsive interactions we establish a minimax principle for the associated mean-field free energy. We show that the phase diagram described by Sonnet *et al.* [Phys. Rev. E **67**, 061701 (2003)] is universal. Our predictions are in good agreement with the recent observations on both V-shaped and tetrapodal molecules.

DOI: 10.1103/PhysRevE.73.051709 PACS number(s): 61.30.Cz, 61.30.Dk

I. INTRODUCTION

Recently, new nematogenic molecules have been synthesized which give rise to thermotropic biaxial phases [1–4]. These experimental findings have revived the interest for macroscopic biaxiality [5,6].

Essentially, two phase diagrams have been so far proposed for biaxial nematics. It is well accepted that macroscopic biaxiality results from anisotropic dispersion forces between biaxial molecules [7]. Excluded-volume effects have also been studied, and—surprisingly enough—for all these different forces the mean-field phase diagram is invariably the same, with a single Landau triple point [8–13]. In the dispersion model, each fluctuating dipole of a molecule interacts with all induced dipoles in another molecule. In general, a dipole of a real molecule always interacts with the corresponding dipole of another molecule, but it may not interact with the other dipoles, which resonate at different frequencies. Ideally, one could think of molecules composed of "independent" oscillators. More recently, a mean-field model has been applied to molecules for which dispersion forces arise from two independent sources [14]. The phase diagram predicted by this model is very different from the one that appeared to be universal: it shows the onset of two tricritical points [15,16]. All previously studied models are peculiar cases of the general Straley quadrupolar interaction potential [8]. The natural question to be asked is then which variety of phase diagrams one could expect to arise from Straley's general interaction. A partial answer has already been given by Longa *et al.* [17]; they showed that the tricritical point found in [14] extends as a line in the parameter space. Here, we complete this study: we show that the two tricritical points found in [15,16] are joined by this line so that the phase diagram presented in [14] describes in full generality the behavior of biaxial liquid crystals within the quadrupolar approximation.

Straley's quadrupolar Hamiltonian for nematogenic biaxial molecules falls within one of two separate classes: it is either *fully attractive* or *partly repulsive*. All are globally attractive Hamiltonians which promote the state where all molecules, depicted as blocks, lie parallel to one another, side by side. Fully attractive Hamiltonians result from the superposition of attractive, purely dispersive interactions. Partly repulsive Hamiltonians result from the superposition of both attractive, purely dispersive interactions and hard-core, repulsive interactions. It has recently been shown that the quadrupolar approximation of the excluded-volume interaction associated with a large class of biaxial molecules introduced by Mulder [18], the sphero-cuboids, is partly repulsive [19]. This class of molecules includes both Straley's blocks [8,10] and sphero-platelets [20,21] as special cases. For all sphero-cuboids, the repulsive component in the effective quadrupolar pair potential is reminiscent of the parent hard-core interaction. It has been conjectured in [19] that the excluded-volume interaction of all biaxial molecules have a partly repulsive quadrupolar approximation.

Classical mean-field theories seeking to minimize an approximate free energy F_0 derived from special, fully attractive, quadrupolar interaction potentials between biaxial molecules have so far been rather successful [8,9,14–16]. However, for partly repulsive potentials the mean-field free energy minimization can lead to paradoxical conclusions, as F_0 may fail to attain its minimum at every stationary point. It is thus necessary to establish a variational principle suited to a general class of potentials that includes the partly repulsive ones.

The minimax principle justified in Sec. II fills this need. In Sec. III, we illustrate the precise notion of partly repulsive Hamiltonian among all general quadrupolar ones. In Sec. IV, we apply the minimax principle to the mean-field approximation to the free energy and, for both fully attractive and partly repulsive interactions, we determine the temperature sequence of stable equilibrium phases. In Sec. V, we compare our predictions with the recent observations of stable biaxial phases exhibited by both V-shaped and tetrapodal molecules. Finally, in Sec. VI we draw the conclusions of our work.

II. MINIMAX PRINCIPLE

The standard strategy to find the stable phases of a system undergoing an ordering transition is to minimize the mean-field approximation F_0 to the free energy F of the system. It is known by example that the presence of repulsive terms in the Hamiltonian can make this strategy fail [22]. For systems described by discrete state variables, a remedy to this failure is known to be the minimax principle first proposed by Bogolubov Jr. in the study of a model problem in superconductivity and later extended to more general spin systems [23,24]. To our knowledge, for systems described by continuous state variables—as are biaxial nematic liquid crystals—no such principle has so far been proposed. This is why, in view of the partly repulsive Hamiltonians encountered in this study, we establish a minimax principle for continuous state variables. Our formulation of this principle is more general than strictly needed here, because it can be applied to a larger class of systems than the one at hand.

Our development builds upon Bogolubov's inequality, which, as shown by Griffiths [25], follows from a general convexity property of the free energy. Let H and H_0 be two Hamiltonians. They give rise to Boltzmann distributions

$$f=\frac{1}{Z}\mathrm{e}^{-H/k_BT} \text{ and } f_0=\frac{1}{Z_0}\mathrm{e}^{-H_0/k_BT}, \tag{1}$$

where T is the absolute temperature, k_B is the Boltzmann constant, and

$$Z=\int \mathrm{e}^{-H/k_BT} \text{ and } Z_0=\int \mathrm{e}^{-H_0/k_BT} \tag{2}$$

are the corresponding partition functions. The integrals in Eqs. (2) must be computed over the appropriate configuration space, which in the case at hand in this paper could be parameterized in terms of the Euler angles. The free energies of the systems described by the Hamiltonians H and H_0 are

$$F=-k_BT\ln Z \text{ and } F_0=-k_BT\ln Z_0, \tag{3}$$

respectively. Bogolubov's inequality states that

$$\langle H-H_0\rangle \leqslant F-F_0 \leqslant \langle H-H_0\rangle_0, \tag{4}$$

where the averages $\langle\cdots\rangle$ and $\langle\cdots\rangle_0$ are computed by using the distributions f and f_0, respectively [25].

We now consider a model for the attractive interaction of two microscopic states $\boldsymbol{q},\boldsymbol{q}'$ in a bounded domain of an n-dimensional inner product space $\mathcal{V}$. For definiteness, $\boldsymbol{q}$ and $\boldsymbol{q}'$ could be identified with specific molecular orientational tensors, as will be done in the following sections. Here, we deliberately keep a higher level of generality to show that the ideas we develop have potentially broader applications. The Hamiltonian is given by

$$H(\boldsymbol{q},\boldsymbol{q}')=-U\boldsymbol{q}\cdot\boldsymbol{q}',$$

where $U>0$ is an interaction energy. As customary [7,26,27], H describes the effective pairwise interactions in a collection of particles, upon averaging over the interparticle vector, and under the assumption that this be isotropically distributed in the ensemble. For example, given a molecule with orientation $\boldsymbol{q}$, the probability of finding another molecule with orientation $\boldsymbol{q}'$ is taken to be the same in all directions. Accordingly, the two-particle distribution function is

$$f(\boldsymbol{q},\boldsymbol{q}')=\frac{1}{Z}\mathrm{e}^{-H(\boldsymbol{q},\boldsymbol{q}')/k_BT}.$$

The corresponding mean-field theory is obtained by replacing the action of $\boldsymbol{q}'$ by an average order parameter $\boldsymbol{Q}$ taken over all states. The mean-field Hamiltonian [24] is

$$H_0(\boldsymbol{q})=-U\left(\boldsymbol{q}-\frac{1}{2}\boldsymbol{Q}\right)\cdot\boldsymbol{Q},$$

and the requirement of self-consistency leads to the compatibility condition

$$\boldsymbol{Q}=\langle\boldsymbol{q}\rangle_0,$$

where the average is taken with respect to the one-particle distribution

$$f_0(\boldsymbol{q})=\frac{1}{Z_0}\mathrm{e}^{-H_0(\boldsymbol{q})/k_BT}.$$

The mean-field averages $\boldsymbol{Q}$ that make this compatibility condition satisfied are precisely those where the mean-field free energy F_0 is stationary.

Both inequalities in (4) are valid for all two-particle distribution functions f; in particular, they apply to the one at thermodynamic equilibrium which minimizes F. Henceforth, we assume that F takes its minimum value and seeks its best approximation F_0. The average of

$$H-H_0=-U\left\{\boldsymbol{q}\cdot\boldsymbol{q}'-\left(\boldsymbol{q}-\frac{1}{2}\boldsymbol{Q}\right)\cdot\boldsymbol{Q}\right\}$$

in the mean-field distribution is readily computed by observing that $\langle\boldsymbol{q}'\rangle_0=\langle\boldsymbol{q}\rangle_0=\boldsymbol{Q}$; one finds that

$$\langle H-H_0\rangle_0=-\frac{1}{2}U\boldsymbol{Q}^2\leqslant 0.$$

Bogolubov's inequality (4) then yields

$$F+\frac{1}{2}U\boldsymbol{Q}^2\leqslant F_0,$$

and the mean-field energy $\frac{1}{2}U\boldsymbol{Q}^2$ can be interpreted as the minimum price to be paid to replace F with F_0. Moreover, F_0, which depends only on the mean-field average $\boldsymbol{Q}$, provides the best approximation to the free energy F wherever it attains its *minimum*.

The situation is less clear cut when the interaction, though globally attractive, has both an attractive and a repulsive part. Let the microscopic state of the system now be represented by a pair $(\boldsymbol{q}^+,\boldsymbol{q}^-)$ of vectors in $\mathcal{V}=\mathcal{V}^+\oplus\mathcal{V}^-$, so that the dimension of $\mathcal{V}$ is $n=n^{+}+n^{-}$. We assume that the interaction Hamiltonian between the microscopic states $(\boldsymbol{q}^{+},\boldsymbol{q}^{-})$ and $(\boldsymbol{q}^{+\prime},\boldsymbol{q}^{-\prime})$ is of the form

$$H = -U(a^{+}\boldsymbol{q}^{+}\cdot\boldsymbol{q}^{+\prime} + a^{-}\boldsymbol{q}^{-}\cdot\boldsymbol{q}^{-\prime}) \tag{5}$$

with $a^{+}>0$ and $a^{-}<0$ chosen so that the ground state of H is at $\boldsymbol{q}^{+\prime}=\boldsymbol{q}^{+}$, $\boldsymbol{q}^{-\prime}=\boldsymbol{q}^{-}$. The corresponding mean-field Hamiltonian is

$$H_0 = -U\left\{a^{+}\left(\boldsymbol{q}^{+}-\frac{1}{2}\boldsymbol{Q}^{+}\right)\cdot\boldsymbol{Q}^{+} + a^{-}\left(\boldsymbol{q}^{-}-\frac{1}{2}\boldsymbol{Q}^{-}\right)\cdot\boldsymbol{Q}^{-}\right\}, \tag{6}$$

where now the two compatibility conditions

$$\boldsymbol{Q}^{+} = \langle\boldsymbol{q}^{+}\rangle_0 \quad\text{and}\quad \boldsymbol{Q}^{-} = \langle\boldsymbol{q}^{-}\rangle_0 \tag{7}$$

must be obeyed.

The average $\langle H-H_0\rangle_0$ is computed as in the purely attractive case; one finds

$$\langle H-H_0\rangle_0 = -g(\boldsymbol{Q}^{+},\boldsymbol{Q}^{-}),$$

where

$$g(\boldsymbol{Q}^{+},\boldsymbol{Q}^{-}) := \frac{1}{2}U(a^{+}\boldsymbol{Q}^{+2} + a^{-}\boldsymbol{Q}^{-2}).$$

Since g can have either sign, the "minimum strategy" may fail to make F_0 as close as possible to F. To devise a better strategy, we also compute the average $\langle H-H_0\rangle$ with respect to the two-particle distribution function. Formally,

$$\langle H-H_0\rangle = -g(\boldsymbol{Q}^{+},\boldsymbol{Q}^{-}) - l(\boldsymbol{Q}^{+},\boldsymbol{Q}^{-}),$$

where

$$\begin{aligned} l(\boldsymbol{Q}^{+},\boldsymbol{Q}^{-}) := U\{&a^{+}(\langle\boldsymbol{q}^{+}\cdot\boldsymbol{q}^{+\prime}\rangle - \langle\boldsymbol{q}^{+}\rangle\cdot\boldsymbol{Q}^{+}) \\ &+ a^{-}(\langle\boldsymbol{q}^{-}\cdot\boldsymbol{q}^{-\prime}\rangle - \langle\boldsymbol{q}^{-}\rangle\cdot\boldsymbol{Q}^{-})\}\end{aligned}$$

is an affine function of $\boldsymbol{Q}^{+}$ and $\boldsymbol{Q}^{-}$. With these definitions, multiplying all terms of inequality (4) by -1 yields

$$g(\boldsymbol{Q}^{+},\boldsymbol{Q}^{-}) \leqslant F_0 - F \leqslant g(\boldsymbol{Q}^{+},\boldsymbol{Q}^{-}) + l(\boldsymbol{Q}^{+},\boldsymbol{Q}^{-}), \tag{8}$$

whence it is apparent that $l\geqslant 0$.

The function $g(\boldsymbol{Q}^{+},\boldsymbol{Q}^{-})$ describes a saddle in the $(\boldsymbol{Q}^{+},\boldsymbol{Q}^{-})$ space, and for any pair $(\boldsymbol{Q}^{+},\boldsymbol{Q}^{-})$ the free energy difference F_0-F lies between that saddle and the one above it described by $g(\boldsymbol{Q}^{+},\boldsymbol{Q}^{-})+l(\boldsymbol{Q}^{+},\boldsymbol{Q}^{-})$.

For each fixed $\boldsymbol{Q}^{-}$, the graph of g is schematically an upward parabola in $\boldsymbol{Q}^{+}$. For $\boldsymbol{Q}^{-}=\boldsymbol{0}$, g is everywhere positive and vanishes only at $\boldsymbol{Q}^{+}=\boldsymbol{0}$; its graph is the highest parabola among all with given $\boldsymbol{Q}^{-}$ (see the lower parabola of the two in Fig. 1). Likewise, for every fixed $\boldsymbol{Q}^{+}$, the graph of g is a downward parabola in $\boldsymbol{Q}^{-}$. Now, the parabola with $\boldsymbol{Q}^{+}=\boldsymbol{0}$ is the lowest among all with given $\boldsymbol{Q}^{+}$; it is everywhere negative and vanishes only for $\boldsymbol{Q}^{-}=\boldsymbol{0}$ (see the lower parabola of the two in Fig. 2).

To locate the stationary points of F_0 that make it as close as possible to F, two strategies seem plausible:

1. Maximin

(a) Minimize F_0 in $\boldsymbol{Q}^{+}$ for fixed $\boldsymbol{Q}^{-}$. At least for $\boldsymbol{Q}^{-}=\boldsymbol{0}$, the minimum of F_0-F is positive (see Fig. 1).

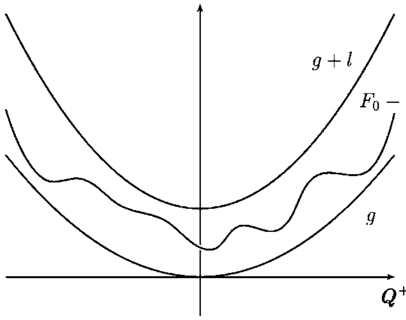

FIG. 1. Free energy difference F_0-F as a function of $\boldsymbol{Q}^{+}$ for $\boldsymbol{Q}^{-}=\boldsymbol{0}$, see Eq. (8).

(b) Take the maximum over all $\boldsymbol{Q}^{-}$ of the minima obtained in step 1(a). This yields the *greatest* of all solutions obtained in step 1(a), which necessarily makes F_0-F positive.

2. Minimax

(a) Maximize F_0 in $\boldsymbol{Q}^{-}$ for fixed $\boldsymbol{Q}^{+}$. At all these maxima, F_0-F is positive; it is so for $\boldsymbol{Q}^{+}=\boldsymbol{0}$, and also for all given $\boldsymbol{Q}^{+}\neq\boldsymbol{0}$, when the graphs of g are parabolas that lie above the lower one in Fig. 2.

(b) Take the minimum over all $\boldsymbol{Q}^{+}$ of the maxima obtained in step 2(a). This yields the *smallest* of all positive solutions obtained in step 2(a), which still makes F_0-F positive.

Since the outcomes of both strategies are positive differences F_0-F, the smallest of all will signal the best F_0 approximating F. Thus, strategy 2 appears to be preferable to strategy 1, and so it becomes the *minimax principle* adopted here. It indicates that while equilibrium states are always distinguished by a minimum of the free energy F, indiscriminate minimization of the mean-field free energy F_0 is not always the best strategy to approximate them.

It is plausible that in general, for systems with either nonquadratic Hamiltonians or discrete state variables, the minimax and the maximin strategies are not equivalent. Here we show that for systems with continuous variables governed by a quadratic Hamiltonian of the form (5) the minimax principle is indeed equivalent to the maximin principle.

Our proof builds upon a local version of the former principle, where local minimax states of F_0 are sought in the appropriate order parameter subspaces: maxima in the repulsive $\boldsymbol{Q}^{-}$ and minima in the attractive $\boldsymbol{Q}^{+}$. Precisely, we prove that every solution of the compatibility conditions (7) is a *local maximum* of F_0 in $\boldsymbol{Q}^{-}$. For fixed $\boldsymbol{Q}^{+}$, we consider $\boldsymbol{Q}^{-}=\boldsymbol{Q}_0+\epsilon\boldsymbol{A}$, where $\boldsymbol{A}$ is an arbitrary vector in $\mathcal{V}^{-}$, $\epsilon\in\mathbb{R}$, and $\boldsymbol{Q}_0$ satisfies the compatibility condition $\boldsymbol{Q}_0=\langle\boldsymbol{q}^{-}\rangle_0$. We define

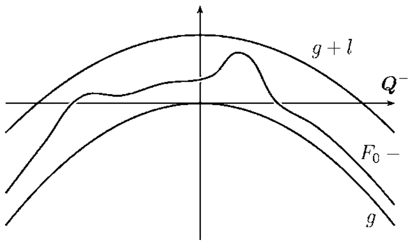

FIG. 2. Free energy difference F_0-F as a function of $\boldsymbol{Q}^{-}$ for $\boldsymbol{Q}^{+}=\boldsymbol{0}$.

$$h(\epsilon) := F_0(\boldsymbol{Q}^+, \boldsymbol{Q}_0 + \epsilon \boldsymbol{A}),$$

where F_0 corresponds to H_0 as in (6). Elementary differentiation then shows that

$$h'(\epsilon) = -k_B T \frac{Z_0'}{Z_0} = \frac{1}{Z_0} \int H_0' \mathrm{e}^{-H_0/k_B T} \mathrm{d}\boldsymbol{q}^+ \mathrm{d}\boldsymbol{q}^- = \langle H_0' \rangle_0, \quad (9)$$

where a prime denotes differentiation with respect to ϵ. Now, $h'(0) = \langle H_0' \rangle_0 = 0$, because $\boldsymbol{Q}_0$ makes F_0 stationary. From (9), the second derivative $h''(0)$ is found to be

$$h''(0) = \langle H_0'' \rangle_0 - \frac{\langle (H_0')^2 \rangle_0}{k_B T}. \quad (10)$$

Since $H_0'' = U a^- \boldsymbol{A}^2$, it follows from (10) that $h''(0) < 0$ for $a^- < 0$. This argument cannot be reversed for the attractive component of the interaction: if the same computation is repeated with all superscripts ± interchanged with ∓, the two terms on the right-hand side of (10) would have opposite sign. Hence, *not* every solution to the compatibility conditions would be automatically a local minimum for F_0 in $\boldsymbol{Q}^+$, while every solution of the compatibility conditions is automatically a local *maximum* in $\boldsymbol{Q}^-$. A general theorem of critical point theory (see Theorem 10.2 of [28]) then ensures that, for every given $\boldsymbol{Q}^+$, there is precisely *one* stationary point of the function $F_0(\boldsymbol{Q}^+, \cdot)$; this makes the maximization of F_0 in $\boldsymbol{Q}^-$ unselective. Thus, the global minimax principle eventually yields the *minimal* value of F_0 over the discrete set of its stationary points. It also follows from the uniqueness of the maximum of $F_0(\boldsymbol{Q}^+, \cdot)$ that the minimax and the maximin principles are equivalent for quadratic Hamiltonians. This latter conclusion is also valid for nonquadratic Hamiltonians H, provided that the approximating Hamiltonian H_0 satisfies $\langle H_0'' \rangle_0 < 0$, see (10). In such a general case, however, a justification for the validity of either minimax or maximin principle as the best strategy to approximate F is at present lacking.

For a class of quadratic Hamiltonians, we proved that both a minimax and a maximin principle provide the best mean-field approximation to the free energy of a system described by continuous microscopic variables. There is a simple criterion to find the local minimax (and maximin) states of F_0. The normal modes of the Hessian form $\mathbb{H}_0$ of F_0 in the whole $\mathcal{V}$ may have components in both spaces $\mathcal{V}^+$ and $\mathcal{V}^-$. Nevertheless, since at a stationary point $\mathbb{H}_0$ is negative definite when restricted to $\mathcal{V}^-$, there must be at least n^- negative eigenvalues of $\mathbb{H}_0$ in $\mathcal{V}$ at all stationary points. Thus, the minimax principle applied to F_0 reduces to labelling as locally stable all equilibria where the largest n^+ eigenvalues of $\mathbb{H}_0$ are positive.

III. QUADRUPOLAR HAMILTONIANS

Biaxial molecules can be described as platelets with a major axis $\boldsymbol{m}$ and two minor axes, $\boldsymbol{e}$ and $\boldsymbol{e}_\perp$. These are the eigenvectors of any molecular polarizability tensor. The anisotropic part of every molecular biaxial tensor has two traceless, orthogonal components, which are defined as

$$\mathbf{q} := \boldsymbol{m} \otimes \boldsymbol{m} - \frac{1}{3}\mathbf{I}, \quad (11a)$$

$$\mathbf{b} := \boldsymbol{e} \otimes \boldsymbol{e} - \boldsymbol{e}_\perp \otimes \boldsymbol{e}_\perp, \quad (11b)$$

where $\mathbf{I}$ is the identity tensor, see [14]. The molecular interaction can be phrased in terms of these tensors. Let two molecules be described by the pairs of tensors $(\mathbf{q}, \mathbf{b})$ and $(\mathbf{q}', \mathbf{b}')$, where $(\mathbf{q}, \mathbf{b})$ and $(\mathbf{q}', \mathbf{b}')$ can in general have different eigenframes. The most general quadrupolar orientational interaction energy H between them, linear in each pair of tensors and invariant under their exchange, takes the form

$$H = -U\{\mathbf{q} \cdot \mathbf{q}' + \gamma(\mathbf{q} \cdot \mathbf{b}' + \mathbf{b} \cdot \mathbf{q}') + \lambda \mathbf{b} \cdot \mathbf{b}'\}, \quad (12)$$

where $U > 0$ is a typical interaction energy and γ and λ are dimensionless parameters. For the ground state of H to lie at $(\mathbf{q}', \mathbf{b}') = (\mathbf{q}, \mathbf{b})$, where the interacting molecules are side by side, γ and λ must satisfy $\lambda - |2\gamma| + 1 > 0$; this inequality is represented by the shaded fan in Fig. 3 [14]. If we only require uniaxial stability of H around the long molecular axis $\boldsymbol{m}$, the whole triangle defined by $\lambda < 0$ and $\lambda - |2\gamma| + 1 > 0$ should be added to this fan (see Fig. 4 below). Here, our attention is confined to the fan, as we only consider possibly biaxial thermotropic phases.

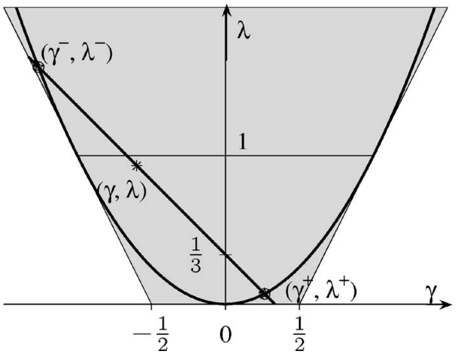

FIG. 3. The shaded fan in the (γ, λ) plane represents the region where H in (12) attains its minimum when $(\mathbf{q}', \mathbf{b}') = (\mathbf{q}, \mathbf{b})$. The points $(\gamma^\pm, \lambda^\pm)$ on the dispersion parabola $\lambda = \gamma^2$ represent the quadratic decomposition (13).

The parabola $\lambda = \gamma^2$ corresponds to the limit with a single quadratic term $H = -U(\mathbf{q} + \gamma\mathbf{b}) \cdot (\mathbf{q}' + \gamma\mathbf{b}')$ suggested by the dispersion forces approximation [7,9,29].

The Hamiltonian (12) can be written uniquely as a superposition of two quadratic components,

$$H = -U(a^+ \mathbf{q}^+ \cdot \mathbf{q}^{+\prime} + a^- \mathbf{q}^- \cdot \mathbf{q}^{-\prime}) \quad (13)$$

with $\mathbf{q}^+$ and $\mathbf{q}^-$ orthogonal molecular tensors, $\mathbf{q}^+ \cdot \mathbf{q}^- = 0$, that represent independent oscillators in the sense explained in the Introduction. For $\gamma \neq 0$,

$$\mathbf{q}^\pm = \mathbf{q} + \gamma^\pm \mathbf{b}$$

with

$$\gamma^\pm = \frac{3\lambda - 1 \pm \sqrt{(3\lambda - 1)^2 + 12\gamma^2}}{6\gamma},$$

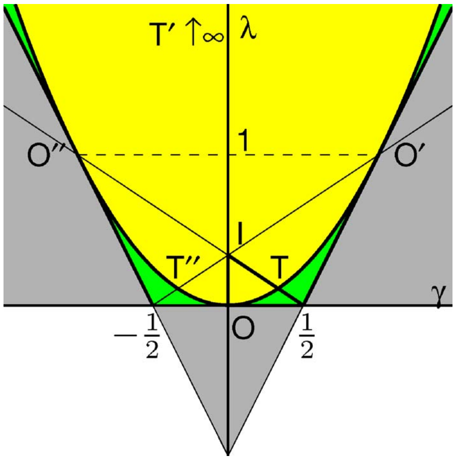

FIG. 4. (Color online) The (yellow) region above the dispersion parabola $\lambda=\gamma^2$ represents fully attractive Hamiltonians, while the (green) region below this parabola represents partly repulsive Hamiltonians. The grey triangle in the half-plane $\lambda<0$ is the region to be added to the fan, if only the stability of molecules around their long axes is required in the ground state. The two other grey regions are conjugated to this triangle via the permutations symmetries of H. O, O′, and O″ represent purely uniaxial interactions. T, T′, and T″ represent purely biaxial interactions. T′ is the point at infinity of the parabola. The lines OT′, O′T″, and O″T represent the permutation symmetries of H; they all meet at the point I.

$$a^+ = \frac{\gamma^- - \gamma}{\gamma^- - \gamma^+}$$

and

$$a^- = \frac{\gamma - \gamma^+}{\gamma^- - \gamma^+}.$$

For $\gamma=0$, $\mathbf{q}^+=\mathbf{q}$, $\mathbf{q}^-=\mathbf{b}$, and $a^-/a^+=\lambda$. The Hamiltonian H in (13) has the general form (5): here $\mathbf{q}^\pm$ belong to isomorphic spaces of dimensions $n^+=n^-=5$.

This decomposition of H can be given a telling geometric interpretation (see Fig. 3). For a given point (γ,λ) representing H in (12), the corresponding points $(\gamma^\pm,\lambda^\pm)$ are the intersections of the parabola $\lambda=\gamma^2$ with the straight line through the points (γ,λ) and $\left(0,\frac{1}{3}\right)$. Thus, all points (γ,λ) on this line are associated with the same roots $\gamma^\pm$, but with different amplitudes $a^\pm$. Imaginatively, if we depict the points (γ,λ) and $(\gamma^\pm,\lambda^\pm)$ as charges, then (γ,λ) is "attracted" by both when $\lambda>\gamma^2$, whereas it is attracted by the closest of the two and "repelled" by the farthest when $\lambda<\gamma^2$.

Equivalently, whenever $\lambda>\gamma^2$ both $a^\pm$ are positive, and so H is decomposed by (13) into two London attractors. On the other hand, whenever $\lambda<\gamma^2$ one of the amplitudes $a^\pm$ is positive and the other is negative, and so H is decomposed by (13) into a London attractor and a London "repulsor," this latter mimicking as in [8] the excluded-volume effects. This repulsion is responsible for the loss of stability of H at the fan boundary.

In short, we say that H is *fully attractive* when $\lambda>\gamma^2$ and *partly repulsive* when

$$\lambda>0, \quad \lambda<\gamma^2, \quad \text{and } \lambda-|2\gamma|+1>0. \tag{14}$$

A notable example of a partly repulsive Hamiltonian is provided by Straley's hard-blocks model [8,10], where H is obtained as the quadrupolar interaction potential that interpolates in selected configurations the pair-excluded volume of parallelepipedes with length L, width W, and breadth B. Both γ and λ in (12) can be expressed in terms of $\ell := L/W$ and $b := B/W$:

$$\gamma = \frac{(\ell^2-b)(b-1)}{2b(1+\ell^2)+2(b^2+\ell^2)-\ell(1+b^2)-6b\ell}, \tag{15a}$$

$$\lambda = \frac{\ell(b-1)^2}{2b(1+\ell^2)+2(b^2+\ell^2)-\ell(1+b^2)-6b\ell}. \tag{15b}$$

The whole admissible region in the (b,ℓ) plane where H has the prescribed ground state is mapped by (15) onto the partly repulsive subregion (14) of the (γ,λ) plane. This is indeed a more general property: the quadrupolar effective pair-potential approximating the excluded-volume interactions of all sphero-cuboids is partly repulsive [19].

IV. PHASE SEQUENCES

In this section, with the aid of the minimax principle illuminated in Sec. II, we determine the sequence in temperature of all stable phases described by the mean-field free energy F_0 associated with the interaction Hamiltonian in Eq. (13).

We use the symmetries induced by the permutations of the molecular axes introduced by Longa *et al.* [17]. For example, the point O, O′, and O″ in Fig. 4 all represent the same interaction energy of equivalent uniaxial molecules with symmetry axes along the molecular frame $(\boldsymbol{e},\boldsymbol{e}_\perp,\boldsymbol{m})$. Similarly, the range of uniaxial stability about $\boldsymbol{m}$, which in Fig. 4 is represented by a triangle in the plane $\lambda<0$, is mapped into the infinite triangles defined by $\lambda>0$ and $\lambda-|2\gamma|+1<0$, when $\boldsymbol{m}$ is replaced by either $\boldsymbol{e}$ or $\boldsymbol{e}_\perp$. As shown in [17], all inequivalent H's are represented by points in the *essential* triangle in Fig. 5 extracted from Fig. 4. All the points conjugated under one of these symmetries should give rise to the same physical behavior, provided the temperature is appropriately rescaled whenever the molecular axis $\boldsymbol{m}$ is involved in the permutation.

The sides of the essential triangle within the fan-region are self-conjugated under permutation symmetries. For each side there is a transformation of the microscopic state that leaves the interaction energy invariant with no associated change in the temperature scale. Thus, a new property arises. Any macroscopic quadrupolar observable $\mathbf{A}$ can be written as a linear superposition of the ensemble averages $\mathbf{Q}$ and $\mathbf{B}$ of $\mathbf{q}$ and $\mathbf{b}$: $\mathbf{A}=\alpha\mathbf{Q}+\beta\mathbf{B}$. The corresponding measurable physical quantities are expressed in terms of their spectra. By imposing the invariance of the spectra under the symmetry transformations that make the Hamiltonian H self-conjugated, we find new constraints on the admissible order tensors $\mathbf{Q}$ and $\mathbf{B}$. The simplest case occurs for $\gamma=0$, where the exchange of $\boldsymbol{e}$ and $\boldsymbol{e}_\perp$ does not change H. By requiring that for $\gamma=0$ the algebraic invariants of $\mathbf{A}^*=\alpha\mathbf{Q}-\beta\mathbf{B}$ be the

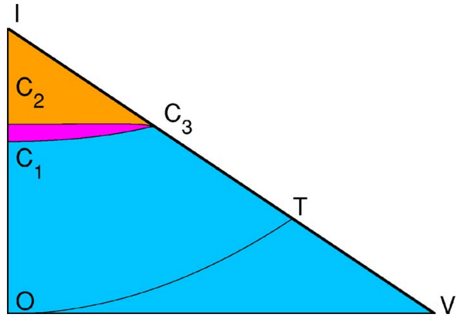

FIG. 5. (Color online) The essential triangle, delimited by thick lines of Fig. 4. The base OV represents Hamiltonians that give rise only to the isotropic-to-uniaxial transition. C$_1$C$_3$ is a tricritical line: the corresponding Hamiltonians produce a phase diagram with a tricritical point along the uniaxial-to-biaxial transition. C$_2$C$_3$ is a triple line: the corresponding Hamiltonians produce a phase diagram with a single direct isotropic-to-biaxial transition, where the isotropic, uniaxial, and biaxial phases are in equilibrium. T is the Landau triple point on the dispersion parabola. C$_3$V is a line of Landau triple points. There, a biaxial phase continuously branches off the isotropic phase.

same as the algebraic invariants of $\mathbf{A}$ for all α and β, we arrive at [30]

$$\mathrm{tr}(\mathbf{QB}) = \mathbf{Q}\cdot\mathbf{B} = 0, \quad \mathrm{tr}(\mathbf{Q}^2\mathbf{B}) = 0, \quad \mathrm{tr}(\mathbf{B}^3) = 0. \qquad (16)$$

In general, $\mathbf{Q}$ and $\mathbf{B}$, which are traceless by construction, are represented in one and the same eigenframe $(\boldsymbol{e}_x, \boldsymbol{e}_y, \boldsymbol{e}_z)$ by four scalar order parameters (S, T, S', T') [8,14],

$$\mathbf{Q} = S\left(\boldsymbol{e}_z \otimes \boldsymbol{e}_z - \frac{1}{3}\mathbf{I}\right) + T(\boldsymbol{e}_x \otimes \boldsymbol{e}_x - \boldsymbol{e}_y \otimes \boldsymbol{e}_y), \qquad (17a)$$

$$\mathbf{B} = S'\left(\boldsymbol{e}_z \otimes \boldsymbol{e}_z - \frac{1}{3}\mathbf{I}\right) + T'(\boldsymbol{e}_x \otimes \boldsymbol{e}_x - \boldsymbol{e}_y \otimes \boldsymbol{e}_y). \qquad (17b)$$

As a consequence of constraints (16), $T = S' = 0$, and so for $\gamma = 0$ all condensed phases can be described by two scalar order parameters, S and T'. Since $\mathbf{Q}$ and $\mathbf{B}$ are orthogonal, one could be tempted to describe the ordered phase by a single tensorial order parameter. This would be misleading because the biaxialities of $\mathbf{Q}$ and $\mathbf{B}$ have different molecular origins: the quadrupolar interactions between the $\mathbf{q}$'s and the $\mathbf{b}$'s are assumed to be independent, and so they cannot be expressed by the interactions of a combined molecular tensor. The constraints in (16) for $\gamma = 0$ have their counterpart on the self-conjugated lines $1 - 3\lambda \pm 2\gamma = 0$, where the phase ordering is again described by two scalar order parameters, conjugated to S and T' [30]; in particular, along side IV of the essential triangle

$$3\,\mathrm{tr}(\mathbf{Q}^2) - \mathrm{tr}(\mathbf{B}^2) - 2\,\mathrm{tr}(\mathbf{QB}) = 0, \qquad (18a)$$

$$\mathrm{tr}(\mathbf{B}^3) - 9\,\mathrm{tr}(\mathbf{Q}^2\mathbf{B}) = 0, \qquad (18b)$$

$$3\,\mathrm{tr}(\mathbf{Q}^3) + 4\,\mathrm{tr}(\mathbf{Q}^2\mathbf{B}) + \mathrm{tr}(\mathbf{QB}^2) = 0. \qquad (18c)$$

Combining condition (18a) with (16), we find that the phase sequence for the intersection I of the three self-conjugated lines is described by a single scalar order parameter, since $S = T'$ for all temperatures. Thus, symmetry requires that if there is any ordering transition at I, this must be a direct first-order isotropic-to-biaxial transition. Had we united S and T' in the same order tensor, we would now arrive at the conclusion that the ordered phase is uniaxial, in contradiction with the result of [14]. Moreover, at the point I the degree of biaxiality of any macroscopic quadrupolar observable is predicted to be independent of the temperature.

We now discuss the sequences of ordered phases for choices of (γ, λ) inside the essential triangle, for both fully attractive and partly repulsive Hamiltonians. In the mean-field approximation, H is replaced by

$$H_0 = -U\left\{a^+\left(\mathbf{q}^+ - \frac{1}{2}\mathbf{Q}^+\right)\cdot\mathbf{Q}^+ + a^-\left(\mathbf{q}^- - \frac{1}{2}\mathbf{Q}^-\right)\cdot\mathbf{Q}^-\right\},$$

where $\mathbf{Q}^+$ and $\mathbf{Q}^-$ are the order tensors defined as

$$\mathbf{Q}^\pm := \langle \mathbf{q}^\pm \rangle_0 = \mathbf{Q} + \gamma^\pm \mathbf{B}. \qquad (19)$$

Here $\langle\cdots\rangle_0$ denotes the ensemble average relative to the mean-field distribution function $f_0(\mathbf{q}^+, \mathbf{Q}^+, \mathbf{q}^-, \mathbf{Q}^-)$, $Z_0(\mathbf{Q}^+, \mathbf{Q}^-)$, and $F_0(\mathbf{Q}^+, \mathbf{Q}^-)$ are the corresponding partition function and free energy, see (1)–(3). The symmetric and traceless tensors $\mathbf{Q}^+$ and $\mathbf{Q}^-$ in general have five independent degrees of freedom each; F_0, which is rotationally invariant, must be a symmetric function of their independent eigenvalues, and so it depends only on four variables (S^+, T^+, S^-, T^-), related to (S, T, S', T') through Eqs. (17) and (19).

We showed in Sec. II that for quadratic Hamiltonians the minimax and the maximin principles provide equivalent strategies to find the best approximation to the minimizer of the free energy F associated with the two-particle Hamiltonian H. For fully attractive Hamiltonians $(a^\pm > 0)$, we minimize F_0 in its four scalar variables. For partly repulsive Hamiltonians $(a^+ > 0, a^- < 0)$, we seek the stationary points of F_0 with minimal energy; these are saddle points of F_0, maxima in (S^-, T^-) and minima in (S^+, T^+).

We performed a numerical bifurcation and continuation analysis of the stationary points of F_0 along straight lines through the vertex $\mathsf{I} = (0, \frac{1}{3})$ of the essential triangle (details will be given elsewhere [30,31]). Along the line $\gamma = 0$, the phase diagram is already known [14] and is governed, as expected, only by two scalar order parameters: it features a tricritical point $\mathrm{C}_1 \simeq (0, 0.20)$ for the uniaxial-to-biaxial transition and a triple point $\mathrm{C}_2 \simeq (0, 0.22)$ between isotropic, uniaxial, and biaxial phases. It follows from [15,16] and the permutation symmetries that along the side IT of the essential triangle there is a tricritical point at $\mathrm{C}_3 = (\frac{5}{29}, \frac{19}{87})$ for the isotropic-to-biaxial transition. Within the essential triangle we find, as in [17], a line of tricritical points that joins C$_1$ and C$_3$. In addition, there is a line of triple points starting from C$_2$ and also ending at C$_3$, where both this line and the tricritical line appear on close inspection to be tangent to the side IT (see Fig. 5). Along the segment IC$_3$ the system undergoes a single first order isotropic-to-biaxial transition [16]. All points of the segment C$_3$T are Landau triple points, but those of the segment IC_3 are not: this corrects the prediction in [17], according to which the whole side IV should consist of Landau triple points.

It should be noted that for partly repulsive Hamiltonians we always find the same phase diagram of [8], which coincides with the one obtained for a single London attractor on the dispersion parabola [9]. The base OV of the essential triangle represents Hamiltonians H for which there exists a single first order isotropic-to-uniaxial transition. This confirms the prediction made in [32] by early Monte Carlo simulations of biaxial systems.

We also explored the segment TV by enforcing constraints (18) on the order tensors $\mathbf{Q}$ and $\mathbf{B}$. Seen in this constrained manifold, TV exhibits only Landau triple points, that is, the corresponding Hamiltonians describe a system that undergoes the isotropic-to-biaxial transition at a single point in the phase diagram, where three phases coexist in equilibrium: isotropic, uniaxial, and biaxial [30].

The phase diagram that was previously considered to be universal extends inside the triangle only up to the tricritical line $\mathsf{C}_1\mathsf{C}_3$. It is characterized by a first-order isotropic-to-uniaxial nematic transition followed, at a lower temperature, by a second-order uniaxial-to-biaxial transition. Between the lines $\mathsf{C}_1\mathsf{C}_3$ and $\mathsf{C}_2\mathsf{C}_3$, we observe the same sequence of phases, but with simple first-order transitions. In the corner of the triangle above the line $\mathsf{C}_2\mathsf{C}_3$ there is only a direct first-order transition between the isotropic and biaxial phases.

A convenient way to represent the universal phase diagram, featuring all the phase sequences described here, is to restrict the molecular parameter space to the boundary OIT of the essential triangle. We call λ^* the arc-length along this folded line. Formally,

$$\lambda^* := \begin{cases} \lambda \in \left[0,\frac{1}{3}\right] & \text{if } \gamma = 0, \\ \frac{1}{3}(1+\sqrt{13}\gamma) & \text{if } \gamma = \frac{1}{2}(1-3\lambda) \in \left[0,\frac{1}{3}\right]. \end{cases} \tag{20}$$

The phase sequences and the corresponding transition temperatures are shown in Fig. 6 against λ^*. The dimensionless temperature $1/\beta^*$ is defined by

$$\frac{1}{\beta^*} := \frac{k_B T}{U^*},$$

where U^* is the condensation energy of the ordered biaxial phase, which is the minimum of H, readily obtained from Eq. (12) as

$$U^* = \frac{2}{3}U(1+3\lambda).$$

As customary, in Fig. 6 broken lines denote second-order transitions and solid lines first-order transitions. In particular, we find that on the segment $\mathsf{C}_3\mathsf{T}$ of all Landau triple points for the fully attractive interactions the maximum transition temperature occurs at T.

Straley [8] put forward the most general quadrupolar molecular interaction, and yet the phase diagram derived from his specific excluded-volume computation did not reveal any of the features discovered here. The reason for this is simple: Straley's excluded-volume interaction Hamiltonian can only be mapped into the partly repulsive region; the associated amplitude U in (13) vanishes along the London dispersion parabola (see Fig. 4) [19].

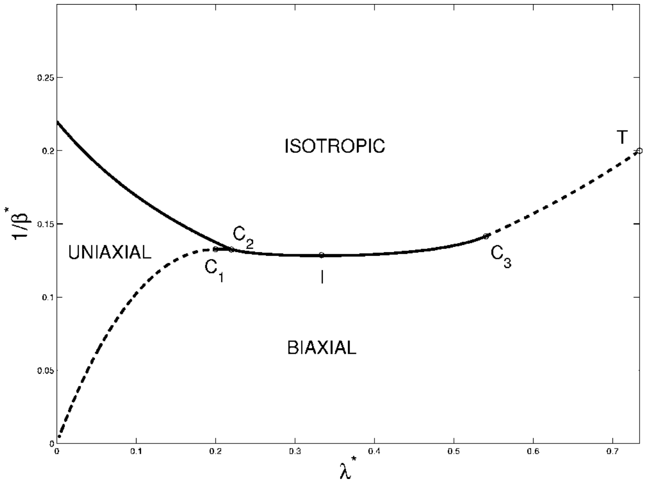

FIG. 6. Universal phase diagram along the boundary OIT of the essential triangle. The parameter λ^*, defined by (20), represents the arc-length along OIT. The tricritical points C_1 and C_3, the triple point C_2, the vertex I, and the Landau triple point T are marked at the values of λ^* where they occur. The dimensionless temperature $1/\beta^*$ is defined by scaling the absolute temperature to the condensation energy U^*, as explained in the text. The temperature of the direct isotropic-to-biaxial transition attains its minimum at I and its maximum at T.

V. DISCUSSION

For experimentalists to observe a stable thermotropic biaxial phase it is essential to choose molecules with fully attractive interactions, which in principle would give rise to a direct isotropic-to-biaxial transition. We know from our study that, to attain the highest transition temperature with attractive interactions, one should choose molecules that interact through the Hamiltonian described by one of the three fully biaxial London points T, T', T'' (see Fig. 4).

This strategy has been quite fruitful. Liquid crystal chemists know very well how to synthesize uniaxial molecules which give rise to large nematic temperature ranges. Making V-shaped molecules using two symmetric identical rodlike arms has been successfully proposed to create a biaxial nematic phase [1,2,33].

Theoretically, the dispersion interaction between the two arms is complete, and so such a molecule is represented by a point on the parabola. By varying the angle θ between the two arms from 0° to 90° the point representing the molecular interaction tensor goes continuously on the parabola from O to O' via T. At O and O' the interaction is uniaxial and associated with the molecular tensors $\boldsymbol{m}\otimes\boldsymbol{m}-\frac{1}{3}\mathbf{I}$ and $\boldsymbol{e}_\perp\otimes\boldsymbol{e}_\perp-\frac{1}{3}\mathbf{I}$, respectively. At T it is purely biaxial and associated with $\boldsymbol{m}\otimes\boldsymbol{m}-\boldsymbol{e}_\perp\otimes\boldsymbol{e}_\perp$. It is easily shown that this corresponds to an angle between the two arms that satisfies $\cos^2\theta = 1/9$, i.e., the two arms are connected at the tetrahedral angle $\theta = 109.47°$ or at $\theta = 70.53°$. In the latter case, the two molecular arms form the sides of an acute triangle, which by itself should not be suited to induce a nematic phase; joining two such co-planar triangles to form an X-shaped molecule would perhaps be a better option. When in a V-shaped molecule the two arms are connected at the tetrahedral angle, the molecule is elongated, and so it is more likely to give rise to a nematic phase. It has also been shown by use of Straley's method that the quadrupolar description of the excluded volume of V-shaped molecules predicts a Landau triple point with a direct transition from the isotropic to the biaxial phase when the inter-arm angle is tetrahedral [12]. This agrees with our findings: Straley's model predicts a Landau triple point when the molecular interaction lies on the segment TV. The Landau triple point reported in [12] must be different from T and should occur at a lower temperature.

Experimentally, the V-shaped molecule that exhibits biaxiality consists of two symmetric arms linked at 140° with a strong transverse central dipole [1,2]. The molecules were boomerang shaped mesogens derived from a 2,5-*bis*-(*p*-hydroxyphenyl)-1,3,4-oxadiazole (ODBP) core. Upon cooling this substance from the isotropic phase, first a transition to a uniaxial nematic phase occurs, followed at a lower temperature by the transition to a stable biaxial. This is coherent with our model. Without the central dipole, the molecular tensor could be described by a point on the parabola away from T because the angle is different from the tetrahedral angle. On the one hand, because of the central dipole, which may not fully interact with the rest of the molecule, the representing point would be attracted inside of the parabola. On the other hand, because of the necessary existence of an excluded volume interaction, it would be pushed outside the parabola. The exact position is inessential, because the phase diagrams close to the parabola are qualitatively the same inside and outside. These arguments remain mostly speculative in nature, as it has not yet been rigorously proved that all V-shaped molecules can be successfully described by the model adopted here.

Another interesting realization of biaxial mesogenic molecules are the tetrapodes employed in [4]. With the aid of two different compounds, experimental evidence of the tricritical point along the uniaxial-to-biaxial transition line was found. This appears to us as the first experimental validation of the universal character of the phase diagram predicted here. It follows from the phase diagram observed in [4] that one of the points representing the molecular interaction energy of the two compounds must lie inside the region $\mathsf{C}_1\mathsf{C}_2\mathsf{C}_3$ in Fig. 5, while the other lies below it. It is plausible that in these tetrapodes the biaxial character is due to the X-shaped central element with high polarizability.

Our model allows to make new predictions for systems composed of independent London oscillators. For instance, since the superposition of two independent uniaxial oscillators of equal strength represented by the points O and O' results in a state described by a point along IT not far from T, another strategy to engineer a nematogenic molecule with biaxial thermotropic phases would be to join at right angles two uniaxial arms, mutually orthogonal and independent.

It would be interesting to find a physical system whose mesogenic molecules would lead to an interaction represented by the point I. Ideally, such a molecule could be realized by joining three completely independent arms at right angles, forming a triple cross as the ones already studied within a pure excluded-volume model [34]. This could be achieved, e.g., by using three independent London oscillators of equal intensity with different frequencies along $\boldsymbol{m}$, $\boldsymbol{e}$, and $\boldsymbol{e}_\perp$. Such a molecule could be almost spherical in shape and not show any excluded volume effect. The first phase to occur upon cooling from the isotropic state could be a plastic crystal with orientational disorder. Upon further cooling we expect to observe a first order transition to a nematic-like biaxial order and, further below, to a fully oriented crystal. It may be that such a system exists and that the first order transition has been mistaken by an ordinary complete crystallization.

VI. CONCLUSIONS

We made a systematic analysis of the phases created by the most general quadrupolar Hamiltonian for anisotropic molecular interactions. Such a Hamiltonian can be either fully attractive or partly repulsive. To find the best mean-field approximation to the free energy of the system, we first extended Bogolubov's minimax principle to continuous state variables. We proved that for quadratic Hamiltonians the minimax and maximin strategies coincide. We applied this method to find the sequence of equilibrium phases in the essential region of the parameter space, for both fully attractive and partly repulsive interactions.

For all attractive interactions, the phase diagram is qualitatively the same as the one found in [14], with the extension to a whole region of the molecular parameter space of both the direct first-order isotropic-to-biaxial transition and a tricritical point. For all partly repulsive interactions, the phase diagram is qualitatively the same as the one predicted in the case of purely London dispersive interactions, with a single Landau triple point marking a second-order isotropic-to-biaxial transition.

Although Straley proposed the most general quadrupolar molecular Hamiltonian adopted here, his excluded-volume model covers only the partly repulsive case. The fully attractive case corresponds physically to pure dispersion forces interactions in the London and McLachlan approximations [35].

This explains why any simulation based on interactions with one London attractor and one London repulsor represented by a quadrupolar Straley's interaction must give qualitatively the same phase diagram with a single Landau triple point, as the one obtained along the dispersion parabola. For decades this has led modelists to believe that this phase diagram is universal. We showed that the most general fully attractive Straley's interaction gives rise to a phase diagram with both a tricritical and a triple point. This phase diagram includes the one obtained along the dispersion parabola as a special case, and so it must be regarded as universal.

Our predictions are in accordance with those made for both purely attractive and partly repulsive interactions of V-shaped mesogenic molecules. The observation of the tricritical point made with the tetrapodal molecules in [4] gives a first validation of the universal character of the phase diagram predicted here.

ACKNOWLEDGMENTS

Financial support from the Royal Society of London through the Project *Biaxial liquid crystals: Mathematical models and simulation* is gratefully acknowledged. We are indebted to M. A. Osipov for an enlightening discussion on the minimax principle originally put forward by N. N. Bogolubov Jr.

[1] L. A. Madsen, T. J. Dingemans, M. Nakata, and E. T. Samulski, Phys. Rev. Lett. **92**, 145505 (2004).

[2] B. R. Acharya, A. Primak, and S. Kumar, Phys. Rev. Lett. **92**, 145506 (2004).

[3] K. Severing and K. Saalwächter, Phys. Rev. Lett. **92**, 125501 (2004).

[4] K. Merkel, A. Kocot, J. K. Vij, R. Korlacki, G. H. Mehl, and T. Meyer, Phys. Rev. Lett. **93**, 237801 (2004).

[5] G. R. Luckhurst, Nature (London) **430**, 413 (2004).

[6] G. R. Luckhurst, Angew. Chem., Int. Ed. **44**, 2834 (2005).

[7] M. J. Freiser, Phys. Rev. Lett. **24**, 1041 (1970).

[8] J. P. Straley, Phys. Rev. A **10**, 1881 (1974).

[9] N. Boccara, R. Mejdani, and L. De Seze, J. Phys. (Paris) **38**, 149 (1976).

[10] B. Mulder, Phys. Rev. A **39**, 360 (1989).

[11] F. Biscarini, C. Chiccoli, P. Pasini, F. Semeria, and C. Zannoni, Phys. Rev. Lett. **75**, 1803 (1995).

[12] P. I. C. Teixeira, A. J. Masters, and B. M. Mulder, Mol. Cryst. Liq. Cryst. Sci. Technol., Sect. A **323**, 167 (1998).

[13] M. A. Bates and G. R. Luckhurst, Phys. Rev. E **72**, 051702 (2005).

[14] A. M. Sonnet, E. G. Virga, and G. E. Durand, Phys. Rev. E **67**, 061701 (2003).

[15] G. De Matteis and E. G. Virga, Phys. Rev. E **71**, 061703 (2005).

[16] G. De Matteis, S. Romano, and E. G. Virga, Phys. Rev. E **72**, 041706 (2005).

[17] L. Longa, P. Grzybowski, S. Romano, and E. Virga, Phys. Rev. E **71**, 051714 (2005).

[18] B. M. Mulder, Mol. Phys. **103**, 1411 (2005).

[19] R. Rosso and E. G. Virga (unpublished).

[20] B. M. Mulder, Liq. Cryst. **1**, 539 (1986).

[21] M. P. Taylor, Liq. Cryst. **9**, 141 (1991).

[22] M. A. Osipov and A. S. Shumovskii, Teor. Mat. Fiz. **46**, 125 (1981) [Theor. Math. Phys. **46**, 83 (1981)].

[23] N. N. Bogolubov Jr., *A Method for Studying Model Hamiltonians* (Pergamon, Oxford, 1972).

[24] N. N. Bogolubov, Jr., B. I. Sadovnikov, and A. S. Shumosky, *Mathematical Methods of Statistical Mechanics of Model Systems* (CRC Press, Boca Raton, 1994).

[25] R. B. Griffiths, J. Math. Phys. **5**, 1215 (1964).

[26] M. J. Freiser, Mol. Cryst. Liq. Cryst. **14**, 165 (1971).

[27] B. Bergersen and P. Palffy-Muhoray, Liq. Cryst. **3**, 347 (1988).

[28] M. Morse and S. S. Cairns, *Critical Point Theory in Global Analysis and Differential Topology* (Academic, New York, 1978).

[29] A. D. Buckingham, in *Intermolecular Forces*, edited by J. O. Hirschfelder (Wiley, London, 1967), Chap. 2 [Adv. Chem. Phys. **12**, 107 (1967)].

[30] G. De Matteis, F. Bisi, and E. G. Virga (unpublished).

[31] F. Bisi, S. Romano, and E. G. Virga (unpublished).

[32] G. R. Luckhurst and S. Romano, Mol. Phys. **40**, 129 (1980).

[33] G. R. Luckhurst, Thin Solid Films **393**, 40 (2001).

[34] R. Blaak and B. M. Mulder, Phys. Rev. E **58**, 5873 (1998).

[35] J. N. Israelachvili, *Intermolecular and Surface Forces* (Academic, London, 1992).